Transportation Research Part C 63 (2016) 114–125

Contents lists available at ScienceDirect

Transportation Research Part C

journal homepage: www.elsevier.com/locate/trc

Geometric design safety estimation based on tire–road side friction

Peiqing Li, Jie He

School of Transportation, Southeast University, No. 2, Sipailou, Nanjing 210096, China

ARTICLE INFO

Article history:
Received 4 March 2015
Received in revised form 8 December 2015
Accepted 16 December 2015
Available online 30 December 2015

Keywords:
Vehicles
Dynamic response
Road geometry
Tire–road side friction
Adams/Matlab

ABSTRACT

A closed-loop drive–vehicle–road–environment system (DVRES) model was established using Adams/Car and Matlab/Simulink. Dynamic responses of lateral tire forces based on tire–road side friction and road geometric characteristics are used to investigate vehicle side slip for geometric design safety estimation. The root mean square, the maximum values of lateral tire forces, comfort limit on curves and vehicle trajectories are used to quantify the safety margin of side friction. The simulation results show that the safety margins of lateral tire forces for radius, operating speed and superelevation rate were 18.2%, 19.3% and 17.6%, respectively, to guarantee good vehicle lateral reliability and ride comfort, while lower speeds are optimal in wet and slippery roads. Finally, a case study was conducted to illustrate the analysis of road design safety, and on-site experiment testing further validated the accuracy and reliability of the closed-loop DVRES model.

1. Introduction

Traffic accidents worldwide are closely related to the interactions between driver, vehicle, road, and environmental factors, such as road geometry, tire–road friction, speeding, vehicle performances, driving behaviors, pavement environments, and traffic flow. However, it is estimated that more than 50% of the total fatalities on highways can be attributed to the accidents occurring on curved sections (Lamm and Choueiri, 1991).

Horizontal curves have a much higher average accident rate than straight segments (Glennon et al., 1985), and this situation is particularly evident in Chinese national highways. Among them, vehicle side slip accident is one of the most frequent on horizontal curves. There are two main reasons. First, a curved section consists of more complex road geometric characteristics and environmental conditions. Second, abrupt changes such as vehicle traveling states, dynamic responses of tire–road friction, and driver visual demands, are more prone to cause driver's improper handling behaviors when a vehicle travels on circular curves and transition sections. Thus, curves and their preceding and succeeding transition sections can be considered as the most critical locations on a highway.

In recent years, a large number of mathematical models and evaluation methodologies were developed to evaluate and analyze traffic safety based on pavement conditions and vehicle reliability. For example, a multiple degrees of freedom vehicle model was established to estimate the interactions between nonlinear tire forces and road friction (Ray, 1997). Due to the loss of vehicle directional stability in emergency maneuvers, a new complete vehicle model based on the linear two-degrees-of-freedom model and tire/road conditions is presented (Mirzaei, 2010). A quarter-car model with two degrees of freedom was used to identify vehicle dynamic behaviors and safe traffic speed limits (Barbosa, 2010). A one-dimensional two-degrees-of-freedom vibration model was formulated to investigate and quantify the effects of pavement roughness

E-mail addresses: lpqing@seu.edu.cn (P. Li), hejie@seu.edu.cn (J. He)

http://dx.doi.org/10.1016/j.trc.2015.12.009
0968-090X/

and vehicle speed (Fuentes et al., 2010). Kang et al. (2013) proposed separate computational methods for evaluating highway alignment according to fuel efficiency, sight distance deficiencies and expected accident costs. The point-mass-model based performance functions considering the failure models of skidding and rollover were presented for a reliability analysis of vehicle stability (You and Sun, 2013). A vehicle vibration and roll model, with seven-degree-of-freedom, was used to analyze the coupling interactions between vehicle anti-rollover and lateral stability (Li et al., 2013). Mirzaeinejad and Mirzaei (2014) used a nonlinear eight-degree-of-freedom vehicle model to optimize the nonlinear control strategy for anti-lock braking system. More recently, driving simulator evaluation is emerging as an important approach for the traffic safety evaluation based on road geometric characteristics, and has demonstrated its usefulness in the road design stage (Bella, 2009; Brown and Brennan, 2015). However, this highlights the fact that no single model is universally acceptable (Jacob and Anjaneyulu, 2012).

As previously mentioned, vehicle models in most literature can be simplified as simple physical models with constant speeds to analyze vehicle dynamic responses. However, these simplified physical models do not accurately reflect the vehicle dynamic responses, especially the dynamic responses of tire–road side friction when the vehicle is traveling on the curves and transition sections. To overcome the above problems, a closed-loop drive–vehicle–road–environment system (DVRES) model, based on virtual prototyping technology, was developed in this study. Currently, virtual prototyping technology has been widely applied to various fields of research, such as the automobile industry, construction machinery, aerospace industry, and mechanical electronics. (Liu and Ma, 2009; Park and Le, 2012; Wong et al., 2013; Daher and Ivantysynova, 2014). Based on an extensive literature review, little work has been undertaken to investigate the vehicle lateral reliability estimation based on tire–road lateral friction and road geometric characteristics using virtual prototyping technology.

Tire–road side friction is an important reference index for identifying potential side slip estimation. When tire–road side friction is insufficient at a horizontal curve, vehicles may side slip, rollover, run off the road, or be involved in head-on accidents. As a result, road design with insufficient tire–road side friction will negate the ability of the driver to guide and control the vehicle in a safe manner. Drivers will also be taken off guard. Accordingly, locations that do not provide vehicle stability can be considered as geometric design inconsistencies, and assessing through vehicle lateral stability can help to identify them.

The closed-loop DVRES model can reflect real car, road geometric characteristics and pavement conditions, and driver maneuvers in the high-fidelity simulator system, and it is possible to reproduce dangerous situations and conditions for the dynamic responses of tire–road side friction. The input variables in the closed-loop DVRES model are radius of R, superelevation rate of e, operating speed of v, and combinations of left and right tire–road friction coefficients of f_l/f_r. Dynamic responses of lateral tire forces are used to identify side slip by analyzing tire force values, vehicle trajectories and traveling states. The root mean square, the maximum values of lateral tire forces, comfort limit (lateral acceleration) on curves and vehicle trajectories are used to quantify the safety margin of side friction.

The aim of this work is to analyze and reveal the traffic accident mechanism of vehicle side slip, and further to optimize the geometric alignment designs. This paper focuses primarily on four sections as follows. Section 2 establishes the closed-loop DVRES model using Adams/Car and Matlab/Simulink, after which, in Section 3, experimental designs and dynamic response analyses for vehicle side slip are formulated. In Section 4, a case study is conducted to improve the geometric alignment designs according to the safety margin of vehicle side slip estimation. Finally the on-site experiment testing further validated the accuracy and reliability of the closed-loop DVRES model.

2. Establishing closed-loop DVRES model

The closed-loop DVRES model consists of three essential components: a full-vehicle model, road model and a control system based on fuzzy rules. A full-vehicle model is composed of the car body, powertrain, front/rear suspension, front/rear tire, brake system and steering etc., in Adams/Car. The road is modeled by Multi-quadric (MQ) interpolation and three-dimensional (3D) road xml file in Adams/Road. The control system is performed by an operating speed profile.

2.1. Three-dimensional road model

The proposed 3D road model is derived from MQ interpolation (Carlson and Foley, 1991; Hon and Mao, 1997). MQ interpolation is one of the best approximation methods in road modeling. The road modeling approach with MQ interpolation can be formulated as follows:

$$F(x) = \sum_{j=1}^{n} a_j \left[(x - x_j)^2 + R^2 \right]^{0.5} \tag{1}$$

$$F(x, y) = \sum_{j=1}^{n} a_j \left[(x - x_j)^2 + (y - y_j)^2 + R^2 \right]^{0.5} \tag{2}$$

where $F(x)$ is one-variable MQ interpolation function, which is applied to handle pavement smoothness and roughness. a_j is an undetermined coefficient. x_j is the j^{th} centerline coordinate scattered on horizontal curve. R is smooth factor. x is interpolation point between x_j and x_{j+1}. $F(x, y)$ is bivariate interpolation function, which is applied to handle 3D road smoothness and elevation.

Without loss of generality, the general form of Eqs. (1) and (2) can be expressed as:

$$y_i = \sum_{j=1}^{n} a_j \left[(x_i - x_j)^2 + R^2 \right]^{0.5} \quad i = 1, 2, \ldots, m \tag{3}$$

$$z_i = \sum_{j=1}^{n} a_j \left[(x_i - x_j)^2 + (y_i - y_j)^2 + R^2 \right]^{0.5} \quad i = 1, 2, \ldots, n \tag{4}$$

Smooth factor R is calculated by empirical equation (see Ding et al., 2005; Sarra, 2006; Zhang and Jiang, 2002 for details), as follow:

$$R^2 = \frac{2}{3} \sum_{i=1}^{n} \sum_{j=1}^{m} \sqrt{(x_i - x_j) + (y_i - y_j)} / (n+1)^2 \tag{5}$$

A 3D road model consists of horizontal alignment, vertical alignment, cross-section, width, superelevation rate, and left/right tire–road contact friction coefficients. That is, the topological structure of a 3D smooth road model can be expressed as vector equation:

$$\mathbf{3D} = [\boldsymbol{x}, \boldsymbol{y}, \boldsymbol{z}, \boldsymbol{w}, \boldsymbol{e}, \boldsymbol{f_l}, \boldsymbol{f_r}] \tag{6}$$

where x, y, z, w, e, f_l, and f_r are denoted as data point coordinates of horizontal alignment, data point coordinates of vertical alignment, data point coordinates of cross-section alignment, road width values, superelevation rates, left tire contact friction coefficient, and right tire contact friction coefficient, respectively.

In the case study, characteristic coordinates $[\boldsymbol{x}, \boldsymbol{y}, \boldsymbol{z}]$ come from the output data of AutoCAD files, in which the appropriate coordinate interval is $[0.1, 5]$ meters for an actual roadway (MSC Software, 2013). The road geometric characteristics $[\boldsymbol{w}, \boldsymbol{e}, \boldsymbol{f_l}, \boldsymbol{f_r}]$ have been set according to an actual roadway features. As a result, the 3D road model can be established according to geometrical characteristics and pavement friction coefficients with Adams/Road, as shown in Fig. 2(a).

2.2. Vehicle model

As shown in Fig. 1, the vehicle is subjected to lateral forces acting at the center of gravity of the vehicle and lateral tire forces when it travels along the horizontal curve.

The lateral force acting at the center of gravity of vehicle based on the point-mass laws of physics is adopted and presented in Eq. (7).

$$F_{lf} = C\cos(\alpha) - G_a \sin(\alpha) \tag{7}$$

with

$$C = \frac{G_a v^2}{gR}$$

where G_a is gravity acting on a vehicle; g is the acceleration due to gravity; v is operating speed; R is radius of curve; and α is superelevation rate.

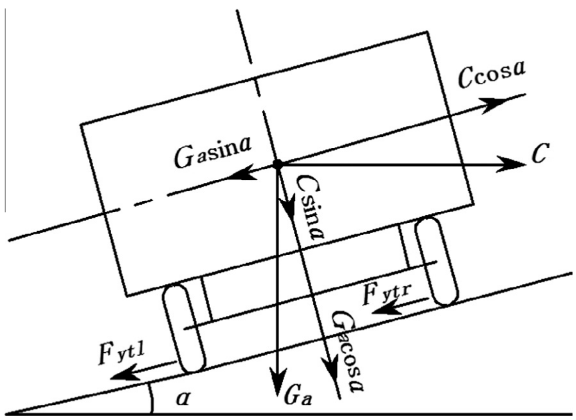

Fig. 1. Vehicle model on a horizontal curve with superelevation.

A general formula of lateral tire force for a car can be written as

$$F_{yt} = F_{ytr} + F_{ytl} = F_{ytrf} + F_{ytrr} + F_{ytlf} + F_{ytlr} \tag{8}$$

where $F_{ytrf}, F_{ytrr}, F_{ytlf}$ and F_{ytlr} are right front lateral tire force, right rear lateral tire force, left front lateral force and left rear lateral tire force, respectively.

An actual vehicle consists of several complex subsystems, such as rigid bodies, flexible bodies, control model and engine system. Therefore, the simplified vehicle models would result in significant discrepancies compared with the real vehicle response especially during extreme driving operations (Li et al., 2013). Overall, the discrepancies mainly ignore vehicle cornering dynamics and inner interactions (You and Sun, 2013). In order to reduce the discrepancies, some key parameters of the HONDA CR-V car were used to establish a vehicle model with Adams/Car. The key parameters of the vehicle are presented in Table 1.

2.3. Tire–road interaction forces and quantification

The contact analyses of tire–road interaction forces can accurately demonstrate the effects on vehicle side slip. Magic-Formula (MF) is used in the vehicle model, named MF tire model; it is considered as the state-of-the-art modeling of the tire–road interaction forces in vehicle dynamic responses (Pacejka, 2005; MSC Software, 2013). The lateral tire force F_y for each tire can be calculated based on the MF empirical equation as follows:

$$\begin{cases} F_y = (D\sin(C\arctan(BX_y - E(BX_y - \arctan(BX_y))))) + S_v \\ X_y = (\alpha + A_9F_Z + A_{10} + A_8\gamma) \\ D = A_1F_Z^2 + A_2F_Z \\ C = A_0 \\ B = \left(A_3\sin\left(2\arctan\frac{F_Z}{A_4}\right) * (1 - A_5|\gamma|)\right) \Big/ \left(A_0 * A_1F_Z^2 + A_2F_Z\right) \\ E = A_6F_Z + A_7 \\ S_v = A_{11}F_Z\gamma + A_{12}F_Z + A_{13} \end{cases} \tag{9}$$

where α is slip angle; γ is inclination angle; F_z is vertical wheel load, and $A_0 \sim A_{13}$ are regression coefficients.

Theoretically, vehicle side slip will occur when the lateral force F_{lf} exceeds the lateral tire force F_{yt}, as shown in Fig. 1. In order to quantify side slip estimation based on tire–road side friction and road geometric characteristics on horizontal

Table 1
Vehicle parameters.

Part	Parameter	Value
Full vehicle	Mass	1625 kg
	Maximum speed	190 km/h
	Length/width/height	4.55/1.82/1.685 m
Car body	Mass	995 kg
	Aero frontal area	1.8 m^2
	Air density	1.2 kg/m^3
	Drag coefficient	0.36
Powertrain	Mass	304 kg
	Max throttle	100
	Final drive	4.11
	Location	Rear
Front suspension	Mass	54 kg
	Type	Macpherson suspension
Rear suspension	Mass	75 kg
	Type	Multi-link suspension
Front/Rear tire	Mass	25 kg
	Stiffness	2.1e+005 N/m
	Damping	50 Ns/m
	Radius	0.344 m
	Width	0.235 m
	Type	MF PAC model
Brake system	Max brake value	100
Steering	Mass	13.2 kg
	Max rack displacement	0.1 m
	Max rack force	10 kN
	Max steering angle	720°

curves, a surrogate measure is proposed, in which both the maximum dynamic lateral tire force and dynamic root-mean-square (RMS) of lateral tire force are calculated and analyzed. The surrogate measures have two advantages: the maximum dynamic lateral tire force can be accurately represented at specific site where side slip accidents may often take place; the RMS dynamic of the lateral tire force can stand for vehicle lateral reliability reference index on a complete horizontal curve. The maximum dynamic lateral tire force F_{max} and the RMS dynamic lateral of tire force F_{RMS} can be calculated as follows:

$$F_{max} = \max(F_{yti}) \quad i = 1, 2, \ldots, n \tag{10}$$

$$F_{RMS} = \sqrt{\frac{F_{yt1}^2 + F_{yt2}^2 + \cdots + F_{ytn}^2}{n}} = \sqrt{\frac{1}{n}\sum_{i=1}^{n} F_{yti}^2} \tag{11}$$

with

$$n = \frac{t_2 - t_1}{T}$$

where F_{yti} is the lateral tire force corresponding to the i-th signal acquisition; n is total number of signal acquisitions on a complete horizontal curve; t_1 is the beginning time of signal acquisition when a vehicle enters a horizontal curve with

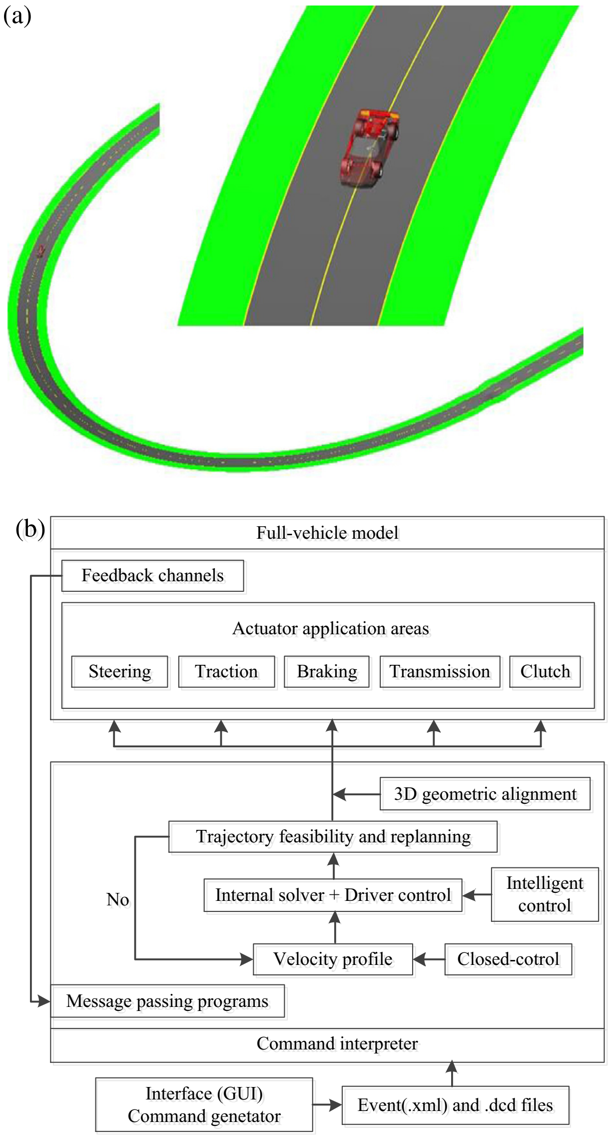

Fig. 2. Integrated closed-loop DVRES model. (a) Dynamic DVRES model; (b) flow chart of closed-loop control system.

superelevation appearance, t_2 is the ending time of signal acquisition when a vehicle exits a horizontal curve with superelevation disappearance, and T is the period of signal acquisition. In following simulation testing, $T = 0.01$.

2.4. Integrated closed-loop DVRES model

The closed-loop DVRES model and control system integrated into the Adams and Matlab/Simulink are specified in flow chart as shown in Fig. 2. In the Closed-Loop DVRES Model, the input parameters are radius, fuzzy-rule-based operating speed profile, superelevation rate, and combinations of right/left pavement friction coefficients. The system outputs are the dynamic responses of lateral tire forces, the traveling trajectories and the vehicle states.

3. Parameter analysis and results

3.1. Effect of radius

Radius is one of the most important geometric parameter for horizontal curves. According to AASHTO (2004) Geometric Design Guideline, the minimum radius of the road is 492 m when the design speed is 100 km/h. Thus, a comparison between six scenarios for different radius parametric studies and numerical quantifications for lateral tire forces are shown in Fig. 3 for $e_{max} = 0.06,\ f_l = f_r = 0.7$.

According to vehicle trajectories, traveling states, comfort limit on curves in DVRES model and numerical quantifications for F_{lf}, F_{max} and F_{RMS}, some conclusions can be drawn: vehicle will rollover when the radii are 200 m and 250 m, respectively; vehicle will side slip and run off the original lane into adjacent lanes when the radii are 300 m and 350 m, respectively; vehi-

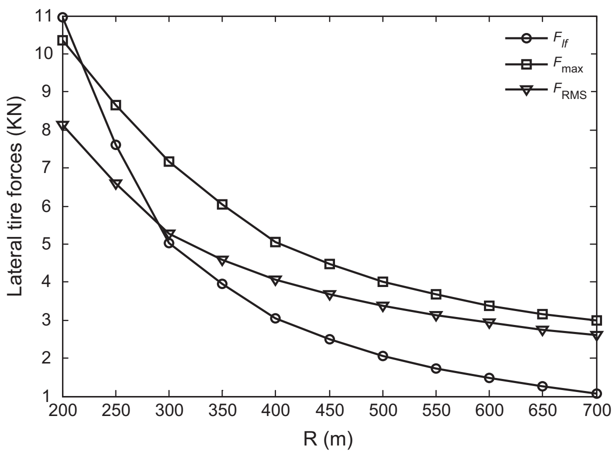

Fig. 3. Effect of radius on lateral tire forces.

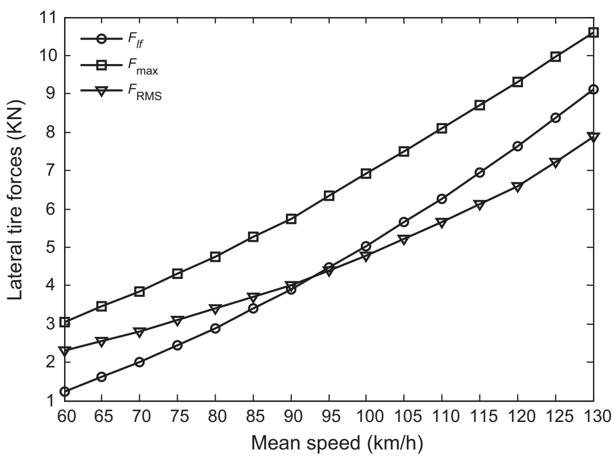

Fig. 4. Effect of speed on lateral tire forces.

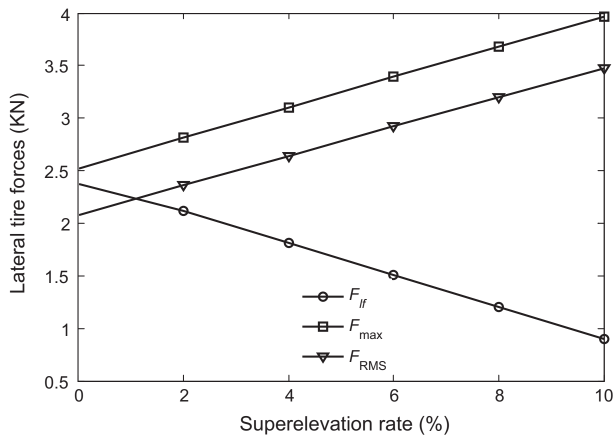

Fig. 5. Effect of superelevation rate on lateral tire forces.

cle have slight side slip without leaving the original lane when the radii are 400 m and 450 m, respectively; vehicle has neither side slip nor rollover when the radii are more than 500 m. In summary, the dynamic responses of the lateral tire forces gradually increase with radii decrease.

3.2. Effect of speed

Federal Highway Administration (FHWA) illustrated that the operating speeds on horizontal curves drops sharply when the radius is less than 250 m (Fitzpatrick et al., 2000). Fig. 4 shows eight scenarios for e_{max} = 0.06, $f_l = f_r = 0.7$.

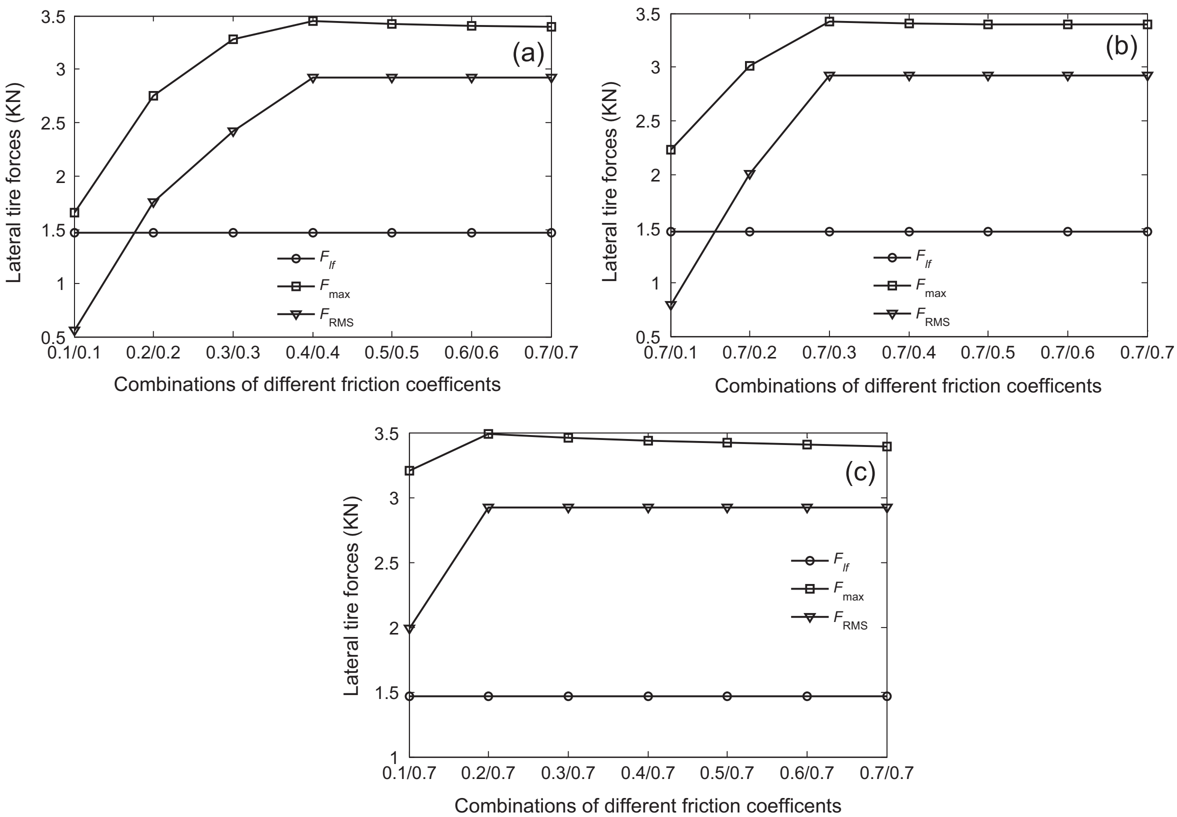

Fig. 6. Effect of friction coefficient on lateral tire forces based on possible combinations of pavement conditions.

According to vehicle trajectories, traveling states, comfort limit on curves in simulation model of the DVRES and numerical quantifications for F_{lf}, F_{max} and F_{RMS}, the following conclusions can be drawn: vehicles will rollover when the operating speeds are 130 km/h and 125 km/h; vehicle suffer side slip and run off the original lane into adjacent lanes when the operating speeds are 120 km/h, 115 km/h, 110 km/h, 105 km/h and 100 km/h, respectively; vehicle experiences side slip and without leaving the original lane when the operating speeds are 90 km/h and 95 km/h; vehicles have neither side slip nor rollover when the operating speeds are more than 85 km/h. In summary, the dynamic responses of the lateral tire forces gradually increase with operating speeds increase.

3.3. Effect of superelevation rate

The superelevation rate is the banking of the pavement on horizontal curves to counteract the effect of the centrifugal force. Fig. 5 provides six scenarios for $R = 500$ m, $v = 100$ km/h $f_l = f_r = 0.7$.

According to vehicle trajectories, traveling states, comfort limit on curves in simulation model of the DVRES and numerical quantifications for F_{lf}, F_{max} and F_{RMS}, the following conclusions can be drawn: vehicle suffered side slip and ran out of the original lane into adjacent lanes when the superelevation rate was 0; vehicles experienced side slip without wandering from the original lane when the superelevation rate was 2; vehicles had neither side slip nor rollover when the superelevation rate was 4. In addition, Fig. 5 shows that the rate of change of lateral tire force in superelevation is nearly constant. Consequently, selecting the appropriate superelevation rate is an effective measure to improve vehicle lateral reliability for driving safety. Therefore, the dynamic responses of the lateral tire forces gradually increase with superelevation rate increase.

3.4. Effect of right/left tire–road friction coefficient

The friction coefficient between tire and road is affected by weather and road conditions. In this paper, dry/wet pavement and road surface unevenness can be considered as the main influencing factors. The pavement friction coefficients are divided into three groups to discuss in terms of possible combinations of pavement conditions as shown in Fig. 6.

Fig. 6(a) represents that the left/right pavement friction coefficient varies from 0.1 to 0.7. Fig. 6(b) represents left pavement friction coefficient varies from 0.1 to 0.7, while right pavement friction coefficient is under dry pavement conditions. The scenario in Fig. 6(c) is opposite to the Fig. 6(b).

The vehicle experienced side slip and rollover when $f_l/f_r = 0.1/0.1, 0.2/0.2, 0.3/0.3, 0.7/0.1, 0.7/0.2$ and $0.1/0.7$, respectively. Fig. 6(a), (b) and (c) show that the rates of change of F_{RMS} and F_{max} without side slip is almost zero, respectively, and it further indicates that side slip is very sensitive to small pavement friction coefficients. Consequently, using lower speeds in wet and slippery road conditions is the optimal choice.

Table 2
Distribution of friction coefficient.

Pavement condition	Mean of friction coefficient	Standard deviation of friction coefficient
Wet and slippery	0.3878	0.0913
Wet and slippery	0.3539	0.0913
Wet and slippery	0.3236	0.0913
Dry and normal	0.8188	0.0949

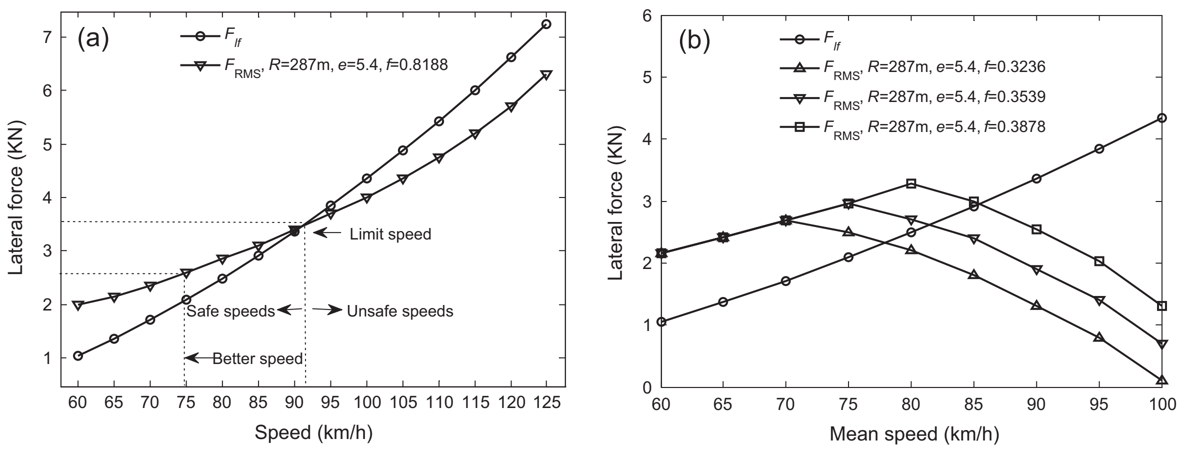

Fig. 7. Dynamic responses of lateral tire forces. (a) Dry and normal pavement; (b) wet and slippery pavement.

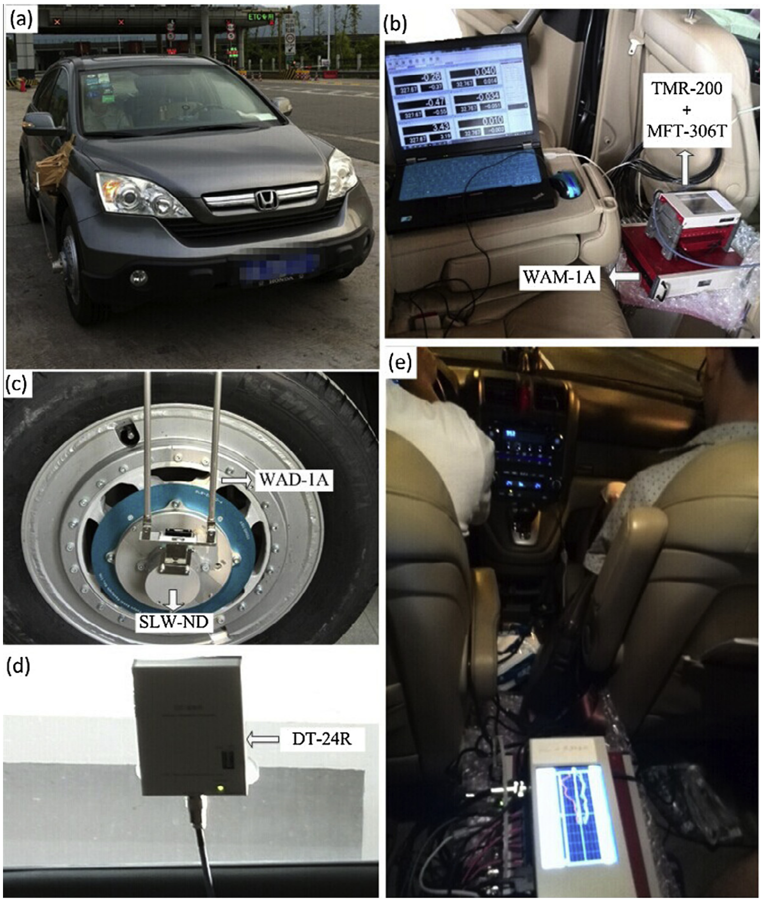

Fig. 8. Experimental setup and testing: (a)–(d) Experimental HONDA CR-V car and automotive instrumentation; (e) field test.

3.5. Results

Based on the analyses and the numerical quantifications for the three parameters, it is evident that the intervals occurred initial side slip for radius, operating speed and superelevation rate are (400500), (80, 90) and (2, 4), respectively. In order to further quantify the vehicle side slip estimation, the following Eq. (12) was used to represent the degree of reliability:

$$\delta = \frac{\Delta F_{sm}}{F_{rl}} * 100\% \tag{12}$$

with

$$\Delta F_{sm} = F_{rl} - F_{rw}$$

where δ is safety margin of lateral tire force F_{RMS}; F_{rl} is the force of $F_{RMS} = F_{lf}$; F_{rw} is the force just without side slip F_{RMS}.

According to vehicle trajectories, traveling states, comfort limit on curves in simulation model of the DVRES and numerical quantifications for F_{lf}, F_{max} and F_{RMS}, the degree of reliability proposed can correctly reflect the safety margin of lateral tire force F_{RMS} within the scope of the vehicle safety threshold, including radius threshold, speed threshold, superelevation rate threshold.

A total of 158 observations (101 observations with radius intervals of 5 meters; 36 observations for every 2 km/h; 21 observations with superelevation rate of 0.5%) are used to calibrate a mathematical model, and In the simulation processing, the safety margin of lateral tire force for radius, operating speed and superelevation **rate were 18.2%, 19.3% and 17.6%, respectively**, which were calculated by first-order one variable linear regression with confident threshold of more than 99.8% and three-order one variable nonlinear regression model with confident threshold of more than 99.8%. Without loss of generality, according to the Technical Standard of Highway Engineering JTG B01—TSHE (MTPRC, 2014), the safety margins of lateral tire force have similar conclusions and the error of safety margin is less than 1.7%, when the radius, speed and superelevation rate change.

Table 3
The driving scenarios for experimental test.

Case	R^a (m)	v^b (km/h)	e^c (%)	f_l/f_r
Case 1	500	79–81	7.3	Dry
Case 2	800	80–82	6.5	Dry
Case 3	650	100–101	6.7	Dry
Case 4	720	98–103	6.9	Dry

According to the analyses of the four parameters above, the dynamic responses of lateral tire forces will be rapidly increased and fluctuate when a vehicle travels with a constant speed in the preceding and succeeding transition sections of a circular curve, respectively. However, the dynamic responses of lateral tire forces in the preceding transition section is significantly greater than that in the succeeding transition section, and the F_{max} also appears in the preceding transition section. This phenomenon implies that there would be a higher probability of vehicle side slip in the preceding transition section than any other. For these reasons, and according to the perspective of vehicle dynamics, the length and radius of curvature in preceding transition section can be appropriately increased to avoid vehicle side slip. For effect of tire–road friction coefficient, using lower speeds in wet and slippery road conditions is the optimal choice.

4. Application

In this section, a case study is given to illustrate the performance of the proposed model, in which Adams and Matlab/Simulink were used to identify and quantify vehicle side slip estimations on horizontal curves.

Taking the G31 Provincial Highway with a superelevation rate 5.4% as example, its design speed is 80 km/h. In Shaoxing city, Zhejiang Province, China, there is a curve with a small radius of 287 m on a section located in hilly and mountainous areas. In the process of vehicle side slip estimation, according to previous research (Lamm et al., 1999; Fambro et al., 2000), the pavement friction coefficients of horizontal curves can be evaluated as shown in Table 2. The dynamic responses of lateral tire forces under different operating speeds conditions are represented as shown in Fig. 7.

Fig. 7(a) shows that the lateral tire force of the posted legal speed limit is about 3.525 kN under dry and normal pavement conditions. However, the lateral tire force should be 2.82 kN after considering the safety margin δ, and in this case, the most appropriate speed should be 75 km/h rather than the design speed of 80 km/h. The G31 Provincial Highway is located in hilly and mountainous areas, so the small radius of R is a significant restriction. Therefore, in order to achieve the design speed of 80 km/h, increased superelevation rate is a better choice to improve the vehicle traveling reliability on the small curve section. Fig. 7(b) shows that the effect of pavement friction coefficient is very sensitive to side slip. Consequently, using lower speeds through a horizontal curve is the optimal choice under wet and slippery road surface conditions.

5. Experimental validation

To further investigate experimentally the performance and accuracy of the closed-loop DVRES model, a detailed comparison between dynamic responses of lateral tire forces obtained from the model and that obtained from field test were made. The field test was performed at different speeds on the Jin-Lin-Wen freeway, which is a segment of G1513 National Highway, in Zhejiang Province, China. The car used was controlled by a driver with more than 10 years of field test driving experience.

5.1. Experimental setup

An experimental HONDA CR-V car and automotive instrumentation are used for the experimental study. Automotive instrumentation consisted of a 6 component force axle load sensor SLW-ND, a wheel alignment measuring system, a wireless signal receiver DT-24R, a 6 component force measuring analyzer MFT-306T, control software WAM-701A, a multifunction car recorder TMR-200 and a Laptop PC. In addition, a wheel alignment measuring system consists of wheel alignment sensor WAD-1A and special measuring analyzer WAM-1A, and the SLW-ND were installed in the right front wheel of the HONDA CR-V car, shown in Fig. 8.

Lateral tire forces were measured by the SLW-ND and then were transferred to the MFT-306T by the DT-24R. The WAD-1A ensured the signal acquisition precision of the SLW-ND, while the WAM-1A ensured the signal processing precision for the WAM-1A.

5.2. Experimental results

Four driving scenarios of experimental testing with different road geometric characteristics and operating speed are detailed illustrated in Table 3

The comparisons between dynamic responses of lateral tire forces obtained from measurement, and those from simulation, are shown in Fig. 9. In order to ensure that the operating speed in the simulation was the same as that in field test, the

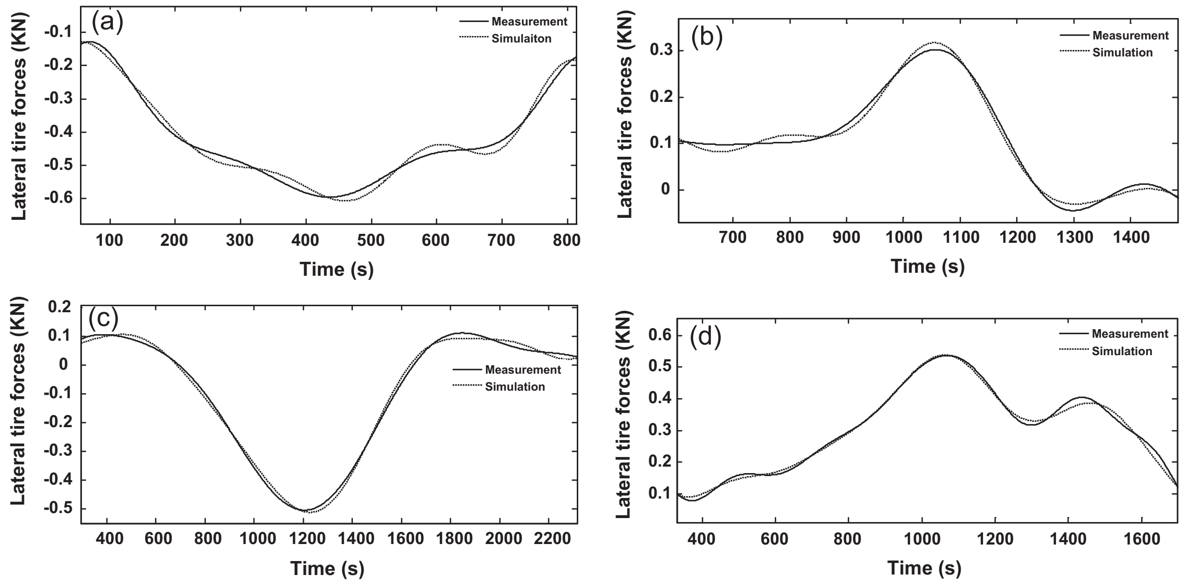

Fig. 9. Lateral tire force of the right front wheel for four situations. (a), (b), (c) and (d) corresponding to case 1, case 2, case 3 and case 4, respectively.

Table 4
Prediction errors between measurement and simulation.

Case	Case 1	Case 1	Case 1	Case 1
RMSE	0.00235	0.00232	0.00231	0.00233
E_{abs}	0.00215	0.00214	0.00212	0.00213

operating speed profiles obtained from the data recorded by automotive instrumentation in the field test were applied to the closed-loop DVRES model. From Fig. 9(a), (b), (c) and (d), it shows that the dynamic responses of lateral tire forces from the field test are sufficiently similar as that of the closed-loop DVRES model in terms of the four cases.

To further demonstrate the performance of the closed-loop DVRES model, an error comparison is made between measurement and simulation. The comparison is shown in Table 4, which lists the root mean square error (*RMSE*) and absolute error (E_{abs}) of the lateral tire force. Among them, the *RMSE* and E_{abs} can be calculated by the following formulae:

$$RMSE = \sqrt{\frac{1}{N}\sum_{i=1}^{n}(y_{pred} - y_{true})^2} \tag{13}$$

$$E_{abs} = \frac{1}{N}\sum_{i=1}^{N}|y_{true} - y_{pred}| \tag{14}$$

where N is the total number of signal acquisitions on a complete horizontal curve, y_{pred} is simulation data and y_{true} is measurement data.

Table 4 shows that the overall percentage error difference is 1.7% between measurement and simulation among them. Therefore, the experimental results further demonstrated the pivotal advantage and potential of the closed-loop DVRES model for practical applicability.

6. Conclusions

In this research, the closed-loop DVRES model was established on the basis of multi-body system dynamics using Adams/Car and Matlab/Simulink. The Magic Formula was applied to calculate the magnitude of dynamic responses of lateral tire forces in the model. The dynamic responses of lateral tire forces were used to investigate vehicle side slip estimations, in which the root mean square and the maximum value are calculated to quantify the safety margin of tire side friction. Finally, on-site experimental testing further validated the accuracy and reliability of the closed-loop DVRES model.

In contrast to simplified physical models, the results show that the proposed analytical model can accurately represent the dynamic responses of lateral tire forces for vehicle side slip estimation on curves. As a result, a slight discrepancy and inconsistency can be observed from dynamic response of lateral tire forces and easily be eliminated by modifying the input variables during the road design stage. For the effects of radius, speed, and superelevation rate, the quantitative results show that the safety margins need to be increased by 18.2%, 19.3% and 17.6%, respectively, to guarantee good vehicle lateral reliability. In contrast, the side slip is very sensitive to small pavement friction coefficients. Thus, using lower speeds through wet and slippery road conditions is the optimal choice.

Finally, further research effort should be devoted to developing other classes of vehicles like passenger cars and heavy trucks and to investigating the lateral stability analysis of vehicle driving safety. In addition, more work is needed to expand the applicability to sections combined horizontal and vertical alignments.

Acknowledgements

The authors would like to thank Education Department of Jiangsu Province (sponsored by Qing Lan Project), and Ministry of Education of China (sponsored by Research Fund for the Doctoral Program of Higher Education of China, Project No. 20120092110044), and Science and Technology Department of Henan Province (sponsored by 2015 key scientific and technical problems, 152102310255). Their assistance is gratefully acknowledged.

References

American Association of State Highway and Transportation Officials, 2004. A Policy on Geometric Design of Highways and Streets, Washington, DC.
Barbosa, R.S., 2010. Vehicle dynamic safety in measured rough pavement. J. Transp. Eng. 137 (5), 305–310.
Bella, F., 2009. Can driving simulators contribute to solving critical issues in geometric design? Transp. Res. Rec. 2138 (1), 120–126.
Brown, A., Brennan, S., 2015. Simulating vehicle dynamics on both design plans and laser-scanned road geometry to guide highway design policy. Transp. Res. Part C 50, 28–36.
Carlson, R.E., Foley, T.A., 1991. The parameter R^2 in multiquadric interpolation. Comput. Math. Appl. 21 (9), 29–42.
Daher, N., Ivantysynova, M., 2014. A virtual yaw rate sensor for articulated vehicles featuring novel electro-hydraulic steer-by-wire technology. Control Eng. Pract. 30, 45–54.
Ding, H., Shu, C., Tang, D.B., 2005. Error estimates of local multiquadric-based differential quadrature (LMQDQ) method through numerical experiments. Int. J. Numer. Meth. Eng. 63 (11), 1513–1529.
Fambro, D., Koppa, R., Picha, D., Fitzpatrick, K., 2000. Driver braking performance in stopping sight distance situations. Transp. Res. Rec. (1701), 9–16
Fitzpatrick, K., Anderson, I., Green, P., Krammes, R., Poggioli, B., 2000. Evaluation of Design Consistency Methods for Two-lane Rural Highways, Executive Summary. Report FHWARD-99-173. Federal Highway Administration, U.S. Department of Transportation, Washington, DC.
Fuentes, L., Gunaratne, M., Hess, D., 2010. Evaluation of the effect of pavement roughness on skid resistance. J. Transp. Eng. 136 (7), 640–653.
Glennon, J.C., Neuman, T.R., Leisch, J.E., 1985. Safety and Operational Considerations for Design of Rural Highway Curves. Federal Highway Administration, U.S. Department of Transportation, Washington, DC.
Hon, Y.C., Mao, X.Z., 1997. A multiquadric interpolation method for solving initial value problems. J. Sci. Comput. 12 (1), 51–55.
Jacob, A., Anjaneyulu, M.V.L.R., 2012. Operating speed of different classes of vehicles at horizontal curves on two-lane rural highways. J. Transp. Eng. 139 (3), 287–294.
Kang, M.W., Shariat, S., Jha, M.K., 2013. New highway geometric design methods for minimizing vehicular fuel consumption and improving safety. Transp. Res. Part C 31, 99–111.
Lamm, R., Choueiri, E.M., 1991. Traffic Safety on Two Continents – A Ten-year Analysis of Human and Vehicular Involvements. No. VTI Rapport 372A, Part 1.
Lamm, R., Psarianos, B., Mailaender, T., 1999. Highway Design and Traffic Safety Engineering Handbook.
Li, Y., Sun, W., Huang, J., Zheng, L., Wang, Y., 2013. Effect of vertical and lateral coupling between tyre and road on vehicle rollover. Veh. Syst. Dyn. 51 (8), 1216–1241.
Liu, H.X., Ma, W., 2009. A virtual vehicle probe model for time-dependent travel time estimation on signalized arterials. Transp. Res. Part C 17 (1), 11–26.
Ministry of Transport of the People's Republic of China, 2014. Technical Standard of Highway Engineering. JTG B01—TSHE Manual, Beijing.
Mirzaei, M., 2010. A new strategy for minimum usage of external yaw moment in vehicle dynamic control system. Transp. Res. Part C 18 (2), 213–224.
Mirzaeinejad, H., Mirzaei, M., 2014. Optimization of nonlinear control strategy for anti-lock braking system with improvement of vehicle directional stability on split-lroads. Transp. Res. Part C 46, 1–15.
MSC Software, 2013. ADAMS Manual.
Pacejka, H., 2005. Tire and Vehicle Dynamics. Elsevier.
Park, H.S., Le, N.T., 2012. Modeling and controlling the mobile harbour crane system with virtual prototyping technology. Int. J. Control Autom. 10 (6), 1204–1214.
Ray, L.R., 1997. Nonlinear tire force estimation and road friction identification: simulation and experiments. Automatica 33 (10), 1819–1833.
Sarra, S.A., 2006. Integrated multiquadric radial basis function approximation methods. Comput. Math. Appl. 51 (8), 1283–1296.
Wong, J.K., Li, H., Wang, H., Huang, T., Luo, E., Li, V., 2013. Toward low-carbon construction processes: the visualisation of predicted emission via virtual prototyping technology. Automat. Constr. 33, 72–78.
You, K., Sun, L., 2013. Reliability analysis of vehicle stability on combined horizontal and vertical alignments: driving safety perspective. J. Transp. Eng. 139 (8), 804–813.
Zhang, Y., Jiang, G.P., 2002. Elastic registration of medical images through multiquadric method. J. First. Mil. Med. Univ. 22 (7), 584–587.